Journal of Electrical Engineering & Technology Vol. 6, No. 4, pp. 527~534, 2011 **527**
DOI: 10.5370/JEET.2011.6.4. 527

Optimization of Powder Core Inductors of Buck-Boost Converters for Hybrid Electric Vehicles

Bong-Gi You*, Jong-Soo Kim*, Byoung-Kuk Lee†, Gwang-Bo Choi and Dong-Wook Yoo*****

Abstract – In the present paper, the characteristics of Mega-Flux®, JNEX-Core®, amorphous and ferrite cores are compared to the inductor of buck-boost converters for Hybrid Electric Vehicles. Core losses are analyzed at the condition of 10 kHz sine wave excitations, and permeability fluctuations vs. temperature and magnetizing force will be analyzed and discussed. Under the specifications of the buck-boost converter for 20 kW THS-II, the power inductor will be designed with Mega-Flux® and JNEX-Core®, and informative simulation results will be provided with respect to dc bias characteristics, core and copper losses.

Keywords: HEVs, Buck-boost inductor, High power density, Low core loss, Thermal stability, Leakage flux.

1. Introduction

Global warming has a close relationship with CO_2 emission and energy consumption. In the light of this issue, vehicles with high fuel efficiency can dramatically reduce CO_2 emission by way of Zero Emission Vehicles and Hybrid Electric Vehicles (HEVs). The appearance of HEVs can be a temporary alternative for eco-friendly vehicles due to the exquisite combination of Internal Combustion engines and electric motors.

In general, HEVs need new components, such as high voltage battery packs, ultra-capacitors, bi-directional dc–dc converters, dc–ac inverters, and electric motors, among others, for the essential mission of enhancing gas mileage. Consequently, this essential mission meets the challenge of designing those new parts as optimized components after considering their qualities in terms of power density, efficiency, reliability, and light weight. Using a minimized number of new components seems to lead vehicles toward achieving good gas mileage. However, Table 1 shows that there is a small trade-off between Toyota Hybrid System (THS) and Toyota Hybrid System II (THS -II), which is the picture of HEVs now.

The main difference between Toyota THS and THS-II is the adoption of a buck-boost converter between the inverter and the battery to realize the "fun to drive" feeling. Compared with THS, which provides 273.6 V_{max}, the boost converter in THS-II provides a power source voltage of 500 V_{max} to the electric motor; this high voltage helps supply the electric motor with lower current and high efficiency [1]. With the boost converter, Toyota has achieved a 50% improvement in motor power output.

Table 1. TOYOTA PRIUS comparison

Quantity	THS (`97 PRIUS)	THS-II (`03 PRIUS II)
HV Battery Voltage	273.6 Vmax (1.2 V x 6-cell x 38 modules)	201.6 Vmax (1.2V x 6-cell x 28 modules)
Power of Motor	33 kW max	50 kW max
Buck/Boost Converter	Not Available	201.6 V ↔ 500 V
Switching Frequency (fs)	Not Available	15 kHz
Max. Torque (N.m)	350	400
Cooling system	10 of above 65 ℃	Uses a coolant

Passive components such as inductors and capacitors often limit total power density and contribute losses. Specifically, the rising temperature of these passive components can change their reliability due to bad thermal environment. Thus, the thermal transfer of passive components and semiconductors is becoming a hot issue in the application of HEVs.

As the power level of the converter reaches 50 kW, high power density packaging then becomes challenging, especially in the application of HEVs due to dc bias characteristics, thermal transfer problems, acoustic noise, and environmental problems, such as vibration and humidity [2]. JFE's JNEX-Core® is typically used in THS-II as the core material of the inductor of the buck-boost converter. JNEX-Core® refers to the non-oriented magnetic steel sheets manufactured by Chemical Vapor Deposition method to increase Si content by 6.5%. Unfortunately, JNEX-Core® needs discrete air gaps to prevent flux

† Corresponding Author: School of Information and Communication Engineering, Sungkyunkwan University, Korea. (bkleeskku@skku.edu)
* School of Information and Communication Engineering, Sungkyunkwan University, Korea.
** R&D Center, Changsung Corporation, Korea.
*** New & Renewable Energy System Research Center, Korea Electrotechnology Research Institute (KERI), Korea.
Received: November 8, 2010; Accepted: April 13, 2011

saturation of the power inductor due to its high permeability, which can make radiated Electro-Magnetic-Interference and induction heating from an astray flux [3]. Amorphous alloy and FINEMET® nanocrystalline from Hitachi and ferrite cores, respectively, also have the same behavior at the point of discrete air gaps. However, Mega-Flux® from Changsung, which has distributed air gapped powder cores composed of Fe-6.5%Si, has similar magnetic behaviors with JNEX-Core® while minimizing the astray flux [4].

In the present paper, as potential candidates for the inductor of the buck-boost converter for HEVs, the characteristics of JNEX-Core®, amorphous crystalline, ferrite cores, and Mega-Flux® are compared in detail. Core losses are analyzed at the condition of 10 kHz sine wave excitation with various flux swing. Permeability fluctuations versus temperature and magnetizing force will also be analyzed and discussed. Under the specifications of the buck-boost converter for 20 kW THS-II, the power inductor will be designed with JNEX-Core® and Mega-Flux®, and informative simulation results will be provided with respect to dc bias characteristics, core and copper losses.

2. Buck/Boost Converter of THS-II

2.1 Power supply system of THS-II

Fig. 1 shows that the boost converter enables THS-II to provide power source voltage of 500 V_{max} to the motor and generator. Meanwhile, the electric motor can yield the same power at the current by 50% compared with a non-boosted case [1].

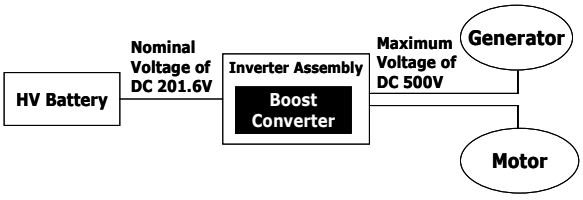

Fig. 1. Buck/Boost Converter Diagram of THS-II

2.2 Buck/Boost converter topology of THS-II

Fig. 2 shows that THS-II uses two switches as its Buck/Boost converter topology.

Mode 1. If the down switch is off, then the main switch is the upper switch that acts as the buck converter. Battery charge mode (500 V → 201.6 V).

Mode 2. If the upper switch is off, then the main switch is the down switch that acts as the boost converter. Driving mode (201.6 V → 500 V).

In Fig. 3, the most severe condition of the power inductor is the moment of starting and accelerating after idling stop. At that time, the current of the power inductor will be at its peak for a few seconds. To get a trade-off design, the following driving profile at Table 2 has been extracted from Fig. 3.

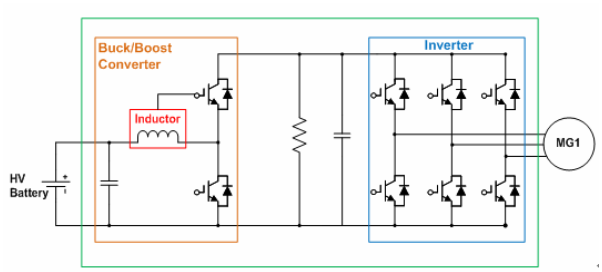

Fig. 2. Buck/Boost Converter Diagram of THS-II

Table 2. Urban Driving Style Portion

Speed	Time	Occupation Rate
0	258 s	18.8%
<10 km/h	89 s	6.5%
10–20 km/h	94 s	6.9%
20–30 km/h	145 s	10.6%
30–40 km/h	265 s	19.4%
40 km/h–	518 s	37.8%
Total	1,369 s	100.0%

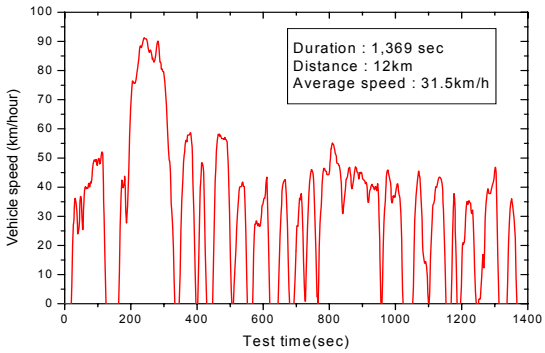

Fig. 3. EPA Urban Dynamometer Driving Schedule

3. Analysis of Core Materials

3.1 The roles of air gap in power inductor

The fundamental purpose of using magnetic cores in a power inductor is to give an easy path for flux in order to save on volume and total efficiency. The main role of the power inductor is to store energy during one portion of each switching period and return this energy to the circuit during another portion of the period as an electric field, which is made from flux swing. The inductance of an inductor is not constant at a given biased current. The effective permeability and slope of the B–H curve are the dominant factors of inductances, and this permeability can be expressed as a function of magnetizing force and initial

permeability (1). Unfortunately, the power inductor can have meaning only when the effective permeability is alive.

$$L = f(u_{eff}, N, A_c, l), \quad u_{eff} = f(u_i, H, B_{sat}) \tag{1}$$

The following equations will show the relationship of air gap effect and magnetizing force.

From Ampere's law:

$$\oint_{closed-path} H \cdot dl = F_c + F_g = ni \left(R_c = \frac{l_c}{\mu \cdot A_c},\ R_g = \frac{l_g}{\mu_0 \cdot A_c}\right)$$

$$ni = \Phi(R_c + R_g) \tag{2}$$

From Faraday's law:

$$V(t) = -n\frac{d\Phi}{dt} = -L\frac{di}{dt} \text{ substitute for } \Phi,\ V(t) = \frac{n^2}{R_c + R_g}\frac{di}{dt}$$

Hence, inductance is

$$L = \frac{n^2}{R_c + R_g} \tag{3}$$

$$\Phi_{sat} = B_{sat} \cdot A_c$$

$$i_{sat} = \frac{B_{sat} A_c}{n}(R_c + R_g) \tag{4}$$

Fig. 4 shows that low permeability and high saturation flux density cores will have great advantages over high permeability and low saturation flux density cores by inserting air gaps in large current applications. There are two methods to insert air gaps in cores. One is to insert bulk air gaps by cutting the path of magnetic flux (Ferrite, JNEX-Core®, FINEMET®, Amorphous strip, and Fe–Si sheet cores), and the other is to make distributed air gaps

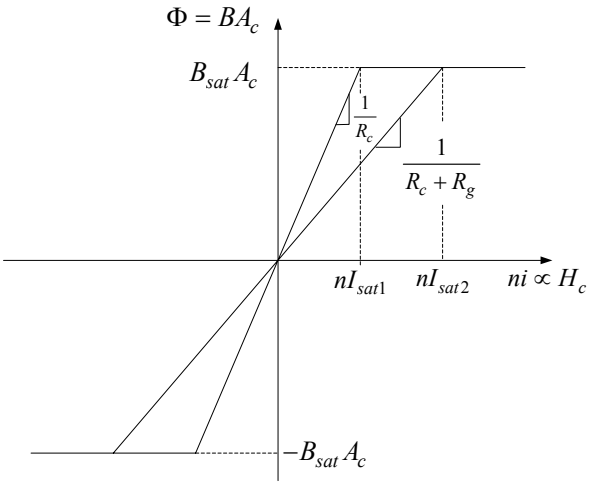

Fig. 4. Air gap effect of the magnetic cores

by insulating metal alloy powders (Mega Flux®, MPP, Sendust, HF, and Iron). Bulk air gap cores have "B: sharp saturation" characteristics, whose permeability rolls off abruptly at the point of saturation level. On the other hand, distributed air gap cores have "A: soft saturation" characteristics, which exhibit a gradual reduction of incremental permeability until, finally, the core is completely saturated (Fig. 5).

Virtually all of the energy is stored in the air gap, so high permeability cores need enough air gaps in their body to store energy. These air gaps are inevitable to enhance the ability of large currents, but they must still be careful with radiated EMI and induction heating. The air gap size also dominates the radius of fringing flux. The larger air gap leads the bigger radius of EMI. There are many potential candidate cores of power inductor in large current applications, particularly the HEVs at Table 3. First, the vehicles must be in the most reliable states, so the following reliability parameters must be satisfactory:

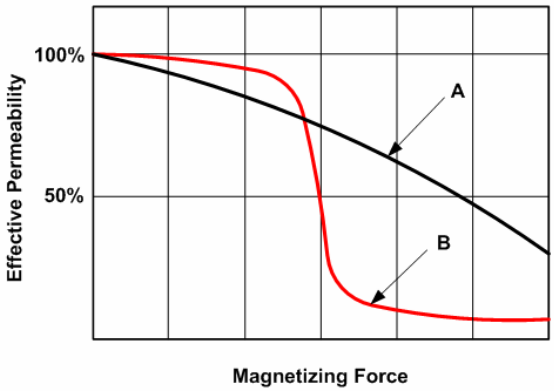

Fig. 5. DC Bias Characteristics

Table 3. Comparison of Core Materials

Class	Material	μ_i	B max [T]	Curie (°C)	*λ (10^{-6})	Fre.	Manufacturer
Powder Core	MPP (Ni-Fe-Mo alloy)	14–550	0.7	450	0	2 MHz	Changsung Magnetics Arnold
	High-Flux (Ni-Fe alloy)		1.5	500	0	1 MHz	
	Sendust (Fe-Si-Al alloy)		1.0	500	0	10 MHz	
	Mega-Flux (Fe-Si alloy)		1.6	725	0.1	10 MHz	
	Iron powder (Fe)	10–75	2.0	770		10 kHz	Micrometals
	Carbonyl Iron	35–50	2.0	770		10 MHz	
Sheet Core	METGLAS 2605SC	3,000	1.5	370	27.0	250 kHz	Hitachi
	METGLAS 2714A	100,000	0.5	205		250 kHz	
	Fe-3%Si (unoriented)	400	1.8	740	7.8	1 kHz	Postech
	Fe-3%Si (oriented)	1,500	1.8	740	-0.8	1 kHz	
	JNEX(Fe-6.5%Si) JNHF(Fe-6.5%Si)	400	1.6	725	0.1	1 MHz	JFE
Ferrite Core	Mn-Zn Ferrite	750–15,000	0.45	250	21.0	2 MHz	TDK FDK
	Ni-Zn Ferrite	10~1,500	0.43	250	21.0	30 MHz	Samwha ISU Ceramic

* Magnetostriction coefficient

- Small and lightweight
- High saturation flux density
- Low core losses at 15 kHz and high flux swing
- Thermal stability
- Minimized radiated EMI
- Long life-time
- Low acoustic noise level

Table 4 shows the comparison of the core materials using the above parameters, and provides an explanation for why JNEX® and Mega Flux® cores are chosen in the present paper.

Table 4. Design Considerations Table

	JNEX®	FINEMET®	Ferrite	Mega-Flux®
Bsat	◎	○	×	◎
Thermal Stability	◎	○	△	◎
EMI	×	×	×	○
Size	◎	○	×	○
Acoustic Noise	○	△	△	◎
Core Loss	○	◎	◎	○

Note : ◎ – Best, ○ – Better, △ – Good, × – Bad.

3.2 Ferrite Cores

Ferrite cores are ceramic materials made by sintering iron oxide with oxides of Mn–Zn or Ni–Zn. Mn–Zn ferrites are widely used in common mode noise filters and 1−2 MHz transformer applications. Ni–Zn ferrites have good frequency reliability from 1 MHz to hundreds MHz due to their high resistivity. Furthermore, ferrite cores are popular in small-powered SMPS for their lower cost and lower loss. However, the saturation flux density (0.45 T) in ferrite is much less than that in metal alloyed cores (0.7−1.8 T). In a large current inductor application, ferrite cores will lead the bulky size to overcome low saturation flux density by inserting large bulk air gaps and large magnetic path length.

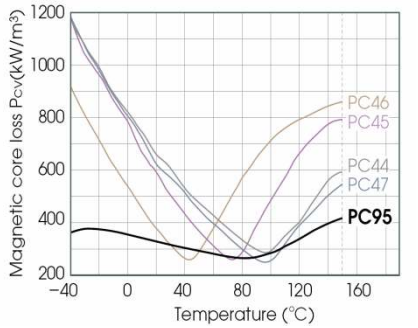

Fig. 6. Ferrite Core Loss versus Temperature (TDK)

Thermally poor characteristics (Fig. 6) make the designer hesitate at environmentally severe applications such as in the military and in vehicles.

3.3 Super cores

The fantastic composition of Fe-6.5%Si is known to possess good magnetic properties in terms of near zero magnetostriction coefficient, high resistivity, and high thermal reliability. Toyota may have adopted JNEX-Core® as its buck/boost inductor for its relative low core loss, thermal reliability, and low acoustic noise level. Meanwhile, this Super Core is under evaluation with THS II. However, there are still risks to emit radiation near field EMI and fringing flux from the bulk air gaps, which are inserted to have good dc bias characteristics. Fig. 7 shows quasi-distributed air gaps in an assembled JNEX-Core®. These quasi-distributed air gaps can minimize the induction heating of heat sink and copper [4].

Fig. 7. JNEX-Core® in THS II

3.4 Amorphous Cores

Amorphous cores are liquid metal strip cores formed by rapid quenching. The amorphous phase has a high resistivity that leads to lower core loss and good frequency stability, but it is a meta-stable state that has a tendency to be crystallized from an amorphous state to a lower energy level if thermal or mechanical energy is added. The crystallization will get rid of their magnetic properties, which explains why amorphous cores have poor thermal stability.

3.4 Mega-Flux Cores

Mega-Flux® cores are made from Fe-6.5%Si alloyed powder, and its distributed air gap structure gives many invisible advantages such as minimized fringing flux, soft saturation, low acoustic noise level, and low core losses. However, their low permeability needs more winding turns than bulky cores, which is caused by too many distributed air gaps for low core losses. The more effective permeability of Mega-Flux® survives at an extremely and highly biased current level.

The high manufacturing pressure of 20 Ton/cm^2 has limited the usage of metal alloy powder cores in large-

current SMPS applications. However, any large-current and high-frequency applications can be designed by stacking powdered Mega Flux® block cores.

4. Simulation Verification

4.1 Core loss versus frequency

Core losses were measured at the condition of 10 kHz sine wave excitations at room temperature and at various magnetic swing flux (IWATSU SY-8217). Fig. 8 shows the core loss comparisons of various core materials. The loss of Ferrite, JNEX-Core®, and FINEMET® will be higher than these data at real application due to the fringing flux [4].

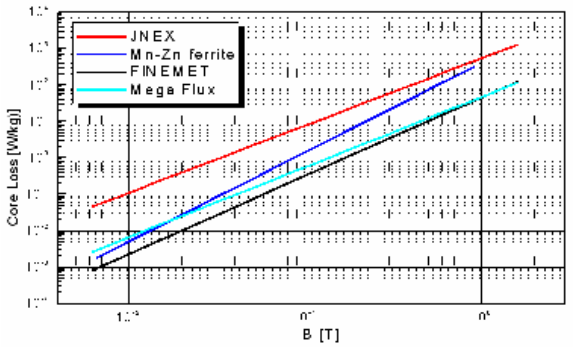

Fig. 8. Core Loss Comparisons

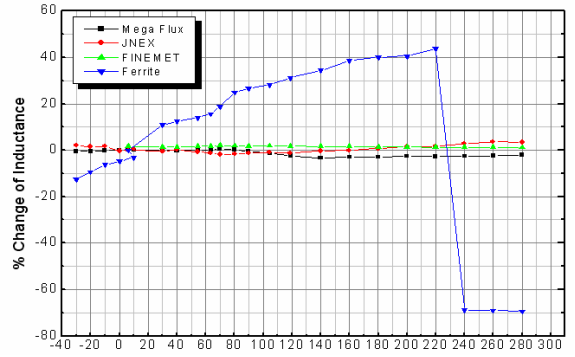

Fig. 9. Temperature Reliability

4.2 Permeability versus temperature

Fig. 9 shows that the permeability of ferrite core changes according to temperature, which means that the saturation flux density of ferrite core is lowered at high temperature due to low Curie temperature.

4.3 Audible noise

Audible noise is mainly due to the magnetostriction coefficient (Table 3). The audible noise spectrum is measured at the condition of 220 V, 60 Hz sine wave and 1 kHz ripple. Mega Flux® shows the lowest acoustic noise performance among Iron powder, JNEX-Core®, and Mega Flux® due to its lowest magnetostriction coefficient and powdered structure (Fig. 10)

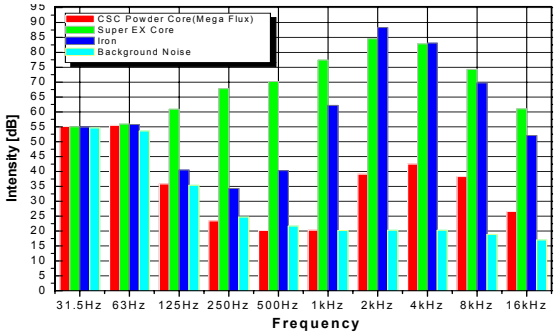

Fig. 10. Spectrum Analysis of Acoustic Noise

4.4 Leakage magnetic flux

Figs. 11 and 12 show that JNEX-Core® has a radiated EMI noise from six pieces of bulk air gaps in the Finite Element Method (FEM). These fringing flux can lead to the malfunction of electronic devices. On the other hand,

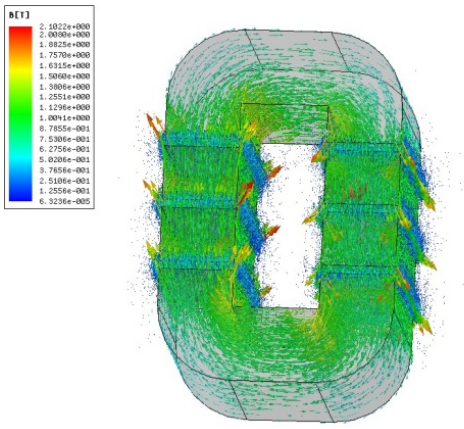

Fig. 11. Magnetic Flux of JNEX-Core®

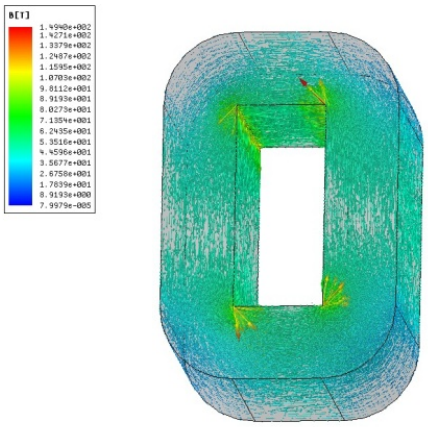

Fig. 12. Magnetic Flux of Mega Flux®

Mega Flux®, which has distributed air gaps in cores, shows little flux leakage.

Several power inductors were designed and manufactured for a 20 kW buck-boost converter for HEVs from the design considerations in Table 3. JNEX-Core® and Mega-Flux® cores were chosen for the design. The detailed buck-boost converter topology is shown in Fig. 2.

Assuming the most severe loading profile at urban driving, the occupation rates of driving states are classified to define the specifications of the velocity of vehicles as shown in Fig. 3. The proposed idea in Table 5 assumes that the buck-boost converter should cover the full power of 20 kW for 13.4% of total driving time (TDT) under the velocity of 20 km/h, a half power of 20 kW for 30% of TDT from 20−40 km/h, and a quarter power of 20 kW for 37.8% of the TDT above 40 km/h (Table 5).

Table 5. Design Specifications and Parameters

Circuit requirements	
Vin → Vout	200 Vdc → 500 Vdc
20 kW (13.4%, ~20 km/h)	100 A (8 s for 1 min)
10 kW (30.0%, ~40 km/h)	50 A (18 s for 1 min)
5 kW (37.8%, 40 km/h~)	25 A (23 s for 1 min)
No load (18.8%, idling stop)	0 A (11 s for 1 min)
Fs	15 kHz
Require Inductance	Min. 200 uH @ 100 A

Table 6. Detailed Parameters of Power Inductors

	JNEX core	Mega-Flux core
Sectional Area (cm^2)	9.0	9.0
Path Length (cm)	20.05	20.05
Core Volume (cc)	157.8	160.7
Core weight (kg)	1.182	1.077
Copper weight (kg)	0.52	0.52

To compare the core materials with ease, power inductors were fabricated with the same core dimension. As mentioned above, six discrete air gaps of 1 mm were inserted in JNEX-Core® [3] to enhance the dc basic characteristics and prevent sharp saturation. Table 6 shows the detailed parameters of buck boost inductors. The dc bias characteristics of JNEX-Core® and Mega-Flux® were tested at the condition of 15 kHz, 1 Volt (HP4284A+ HP42841A). Informative simulations were carried out as the proposed driving profile with the results summarized in Table 7. With dielectric losses and other stray losses being omitted, the total power inductor losses are the sum of the core and winding losses. Simulation results show that the average losses of Mega-Flux® are lower than JNEX-Core® by 32.2 Watt; however, these numerical values can be variable according to different driving profiles and discrete air gap sizes. Moreover, copper losses of JNEX-Core® and Mega Flux® are almost the same because they have the same number of turns and wire area. With the high inductance of Mega-Flux®, the inductor losses are then lower than JNEX-Core® at a low load profile. The dc bias characteristics of JNEX-Core® exceed Mega-Flux® from 55 A, but the reversal of Mega-Flux® occurs after 250 A as shown in Fig. 13.

Table 7. Total Loss Calculation of Power Inductor

Driving time (@ 60 s)		8 s	18 s	23 s
Load Current (A)		100	50	25
Fs		15 kHz	15 kHz	15 kHz
JNEX-Core®	L(uH) at Load	350	360	370
	Ripple Current (A)	22.9	22.2	21.6
	Peak Current (A)	111.4	61.1	35.8
	Flux Swing (T)	0.204	0.198	0.193
	Core Loss × Duration Time (Ws)	472.8	1,063.8	1,359.3
	Copper Loss × Duration Time (Ws)	1,552.0	873.0	278.3
	Average Loss(W)	93.3		
Mega Flux®	L(uH) at Load	220	370	450
	Ripple Current (A)	36.4	21.6	17.8
	Peak Current (A)	118.2	60.8	33.9
	Flux Swing (T)	0.325	0.193	0.159
	Core Loss × Duration Time (Ws)	395.2	306	262.2
	Copper Loss × Duration Time (Ws)	1,552.0	873.0	278.3
	Average Loss(W)	61.1		

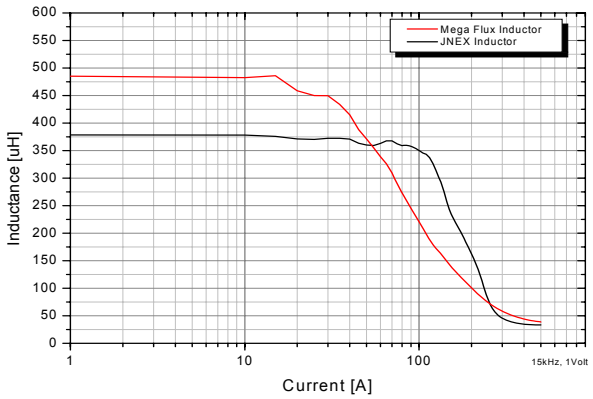

Fig. 13. Characteristic of DC Bias

Fig. 14. Prototype of Mega Flux® Inductor

5. Conclusion

Potential candidates for core materials that can be used to make power inductors for HEVs were analyzed. The

simulation results of both JNEX-Core® and Mega-Flux® cores satisfy the following requirements for HEVs: high saturation flux density, low core losses above 15 kHz, thermal stability, and low acoustic noise level. However, JNEX Core® will have leakage flux and radiated EMI from the discrete bulk air gaps. On the other hand, the distributed air-gapped Mega-Flux® will be strong at astray losses and radiated EMI problems. Thus, to examine dielectric and astray losses, FEM was also performed. As observed, the "soft saturation" of Mega-Flux® can give high efficiency at light load and high reliability at full load condition. From the core losses versus frequency, Mega-Flux® will have more advantages at a higher switching frequency of 15 kHz with the lower core losses. Two JNEX-Core® and Mega Flux® inductors were built and experimentally evaluated, and it was found that metal-alloyed powdered structure inductors such as Mega Flux® could be optimally designed for electric vehicle applications.

Acknowledgment

This work was supported by the Human Resources Development (20104010100630-11-1-000) of the Korea Institute of Energy Technology Evaluation and Planning (KETEP) grant funded by the Korean Government's Ministry of Knowledge Economy

References

[1] Toyota Motor Corporation, "TOYOTA PRIUS Manual," No. NCF255U, August, 2003.
[2] M. Ehsani, K. M. Rahman, M. D. Bellar, A. Severinsky, "Evaluation of soft switching for EV and HEV motor drives," IEEE Trans. on Industrial Electronics, vol. 48, no. 1, pp. 82-90, Feb., 2001.
[3] M. Gerber, J. A. Ferreira, "A high-density heat-sink-mounted inductor for automotive applications," IEEE Trans. on Industrial Electronics, vol. 40, no. 4, pp. 1031-1038, July/Aug., 2004.
[4] T. E. Salem, D. P. Urciuoli, V. Lubomirsky, G. K. Ovrebo, "Design considerations for high power inductors in dc-dc converters," 22nd Annual IEEE Applied Power Electronics Conference and Exposition, pp. 1258-1263, Feb./Mar., 2007.
[5] F. Liffran, "A procedure to optimize the inductor design in boost PFC applications," 13th Power Electronics and Motion Control Conference, pp. 409-416, Sept., 2008
[6] T. Saito, S. Takemoto, T. Iriyama, "Resistivity and core size dependencies of eddy current loss for Fe-Si compressed cores," IEEE Trans. on Magnetics, vol. 41, no. 10, pp. 3301-3303, Oct., 2005

Bong-Gi You received his B.S. degree in Ceramic Engineering from Yonsei University, Seoul, Korea in 1999 and his M.S. in Electrical Engineering from Sungkyunkwan University, Suwon, Korea, in 2011. Since 1999, he has worked for Changsung Corporation as an application and marketing engineer. His research interests include soft magnetic materials, electro-magnetic simulation, inductor design, renewable energy source modeling, high power DC–DC converter for PHEV/EV, battery chargers for PHEV/EV, and interleaved DC–DC converters.

Jong-Soo Kim received his M.S. degree in Electrical Engineering from Sungkyunwan University, Suwon, Korea, in 2008. Since 2008, he has worked for his Ph.D. in Electrical Engineering at Sungkyunwan University. His research interests include eco-friendly vehicle technologies, power conditioning systems for renewable energy, and PM motor drives.

Byoung-Kuk Lee received his B.S. and M.S. degrees in Electrical Engineering from Hanyang University, Seoul, Korea, in 1994 and 1996, respectively, and his Ph.D. from Texas A&M University, College Station, TX, USA in 2001. From 2003 to 2005, he was a Senior Researcher at the Power Electronics Group, KERI, Changwon, Korea. In 2006, he joined the School of Information and Communication Engineering, Sungkyunkwan University, Suwon, Korea, as an Assistant Professor. His research interests include electric vehicles, sensorless drives for high-speed PM motors, power conditioning systems for renewable energy, modeling and simulation, and power electronics.

Prof. Lee is a recipient of the Outstanding Scientists of the 21st Century from IBC and is listed in the 2008 62nd edition of "Who's Who in America" and in the 2009 26th edition of "Who's Who in the World." Prof. Lee is an Associate Editor in the IEEE Transactions on Industrial Electronics and an IEEE Senior Member.

Gwang-Bo Choi received his B.S. and M.S. degrees in Metallurgical Engineering from Seoul National Univerity, Seoul, Korea, in 1988 and 1990, respectively, and his Ph.D. from Yonsei University, Seoul, Korea in 2005. Since 1990, he has worked for the R&D Center of Changsung Corporation. His research interests include soft magnetic materials, powder technology, material processing, and power industries for EV and UPS.

Dong-Wook Yoo received his B.S. degree in Electrical Engineering from Sung-Kyun-Kwan University (SKKU), Suwon, Korea, in 1983, his M.S. degree in Electrical Engineering from Yon-Sei University, Seoul, Korea, in 1985, and his Ph.D. degree with specialization in Power Electronics from SKKU in 1997.

He worked at the Korea Electrotechnology Research Institute (KERI), Changwon, Korea, where he was a Researcher in 1985, a Senior Researcher in 1989, and a Principal Researcher in 1997. Since 1997, he has been a Team Leader at the Power Electronics Laboratory and Renewable Energy Laboratory of the Korea Electrotechnology Research Institute in Changwon, Korea. He has authored or coauthored more than 20 publications in IEEE Transactions, and holds more than 40 Korean patents, including six U.S. patents. Dr. Yoo is a member of the IEEE Power Electronics Society, IEEE Industry Applications Society, Korean Institute of Power Electronics Society (KIPE), and Korean Institute of Electrical Engineers (KIEE).

In 2005 and 2009, he was the Chairman of the KIPE conference, and is currently the Vice President. He was a co-recipient of the 2002 Annual Conference of the IEEE Industrial Electronics Society Best Paper Awardand the 2007 International Conference on Power Electronics Best Paper Award in Daegu, Korea.